DOI: 10.1002/cplu.200

Functionalized Dithienylthiazolo[5,4-*d*]thiazoles for Solution-Processable Organic Field-Effect Transistors

Sarah Van Mierloo,[a] Karolien Vasseur,[b] Niko Van den Brande,[c] Ayse E. Boyukbayram,[a],[d] Bart Ruttens,[e] Silvio D. Rodriguez,[f],[g] Edith Botek,[f] Vincent Liégeois,[f] Jan D'Haen,[e] Peter J. Adriaensens,[a] Paul Heremans,[b] Benoît Champagne,[f] Guy Van Assche,[c] Laurence Lutsen,[h] Dirk J. Vanderzande,* [a],[h] and Wouter Maes* [a],[i]

A series of 5'-aryl-substituted 2,5-bis(3'-hexylthiophen-2'-yl)thiazolo[5,4-*d*]thiazole derivatives was synthesized and these expanded semiconductors were investigated as active materials for solution-processable organic field-effect transistors. Field-effect mobilities up to 10^{-3} cm^2 V^{-1} s^{-1} were obtained, representing the first reasonable FET behavior for highly soluble thiazolo[5,4-*d*]thiazole-based small organic compounds suitable for printable electronics. Thermal and electro-optical material properties were studied by thermogravimetric analysis, differential scanning calorimetry, cyclic voltammetry and UV-vis spectroscopy. Trends in thermal and optical data were supported by (time-dependent) density functional theory calculations. Additional X-ray diffraction, atomic force microscopy and scanning electron microscopy studies provided insight in the relationship between the molecular structures, film morphologies and FET performances. The fibrillar microcrystalline structure observed for the best-performing thienyl-substituted material was linked to the high mobility.

Introduction

Organic semiconductors recently receive significant attention as functional materials applicable in organic field-effect transistors (OFET's),[1] organic light emitting diodes (OLED's),[2] and organic photovoltaics (OPV).[3] Some of the particular features of organic materials render them more attractive than their inorganic counterparts for electronic applications requiring large area coverage, structural flexibility and solution processability. In the design of organic semiconductors, the consideration of molecular properties such as oxidation potentials, electron affinities and intermolecular *π*-*π* interactions is a crucial aspect. Several prominent semiconducting materials have been obtained by structural modifications of oligothiophene derivatives and their properties have been tuned by introducing particular substituents onto the *π*-conjugated backbone.[4] Among these thiophene-based (small) molecules, a number of materials containing a thiazolo[5,4-*d*]thiazole (TzTz) unit have shown high field-effect mobilities when used as active layers in both *n*- and *p*-type OFET devices. The TzTz fused heterocycle shows some excellent characteristics toward applications in organic electronics. Its electron-accepting character enhances the stability of the resulting materials toward oxygen. TzTz compounds are generally stable under ambient atmosphere at room temperature over a period of several months. Moreover, the TzTz moiety has a rigid planar structure due to the fused bicyclic ring system, which leads to efficient intermolecular *π*-*π* interactions.[5–7] Finally, 2,5-diaryl-substituted TzTz's can easily be synthesized starting from the corresponding arylcarbaldehydes and dithiooxamide.[8,9]

The majority of TzTz molecules reported so far is very poorly soluble and requires vacuum deposition techniques for device fabrication. In order to be applicable to printing processes, highly attractive for large area coverage at a reasonable cost, solubilizing groups/side chains have to be appended to the extended *π*-system. Such highly soluble TzTz materials are also of particular appeal for integration (as acceptor components) in low bandgap donor-acceptor copolymers toward efficient organic solar cells. The interest in the TzTz structure in this respect has increased spectacularly, noticeably in the last year.[10]

In this paper, a series of highly soluble functionalized TzTz-based semiconductors is presented. Four 2,5-bis-(5'-aryl-3'-hexylthiophen-2'-yl)thiazolo[5,4-*d*]thiazole (DTTzTz) molecules, i.e. **Th-DTTzTz**, **4-CF_3-Ph-DTTzTz**, **4-F-Ph-DTTzTz** and **4-CN-Ph-DTTzTz** (Scheme 1), were synthesized, in which the two 3-hexylthiophene units ensure solvent-based processing.[11] Functionalization, purification and characterization of the molecules are considerably simplified by their high solubility. The correlation between the molecular structures of the synthesized DTTzTz derivatives, their thermal and (photo)physical properties, spin-coated film morphologies and FET performances was thoroughly analyzed.

[a] *Dr. S. Van Mierloo, Dr. A. E. Boyukbayram, Prof. Dr. P. J. Adriaensens, Prof. Dr. D. J. Vanderzande, Prof. Dr. W. Maes*
Design & Synthesis of Organic Semiconductors (DSOS)
Hasselt University, Institute for Materials Research (IMO-IMOMEC)
Agoralaan 1 - Building D, B-3590 Diepenbeek, Belgium
E-mail: dirk.vanderzande@uhasselt.be, wouter.maes@uhasselt.be
[b] *K. Vasseur, Prof. Dr. P. Heremans*
IMEC
Kapeldreef 75, B-3001 Leuven, Belgium
Department of Metallurgy and Materials Engineering
KU Leuven
Kasteelpark Arenberg 44, B-3001 Leuven, Belgium
[c] *N. Van den Brande, Prof. Dr. G. Van Assche*
Department of Materials and Chemistry, Physical Chemistry and Polymer Science
Vrije Universiteit Brussel
Pleinlaan 2, B-1050 Brussels, Belgium
[d] *Dr. A. E. Boyukbayram*
Department of Chemistry
Karabuk University
78000 Karabuk, Turkey
[e] *B. Ruttens, Dr. J. D'Haen*
Electrical and Physical Characterization (ELPHYC)
Hasselt University, Institute for Materials Research (IMO-IMOMEC)
Universitaire Campus - Wetenschapspark 1, B-3590 Diepenbeek, Belgium
[f] *S. D. Rodriguez, Dr. V. Liégeois, Dr. E. Botek, Prof. Dr. B. Champagne*
Laboratoire de Chimie Théorique
Facultés Universitaires Notre-Dame de la Paix (FUNDP)
Rue de Bruxelles 61, B-5000 Namur, Belgium
[g] *S. D. Rodriguez*
Medio Ambiente y Energía
Instituto de Química-Física de Materiales, Universidad de Buenos Aires
Pabellón II, Ciudad Universitaria, C1428EGA Buenos Aires, Argentina
[h] *Dr. L. Lutsen, Prof. Dr. D. J. Vanderzande*
IMEC, IMOMEC Ass. Lab.
Universitaire Campus - Wetenschapspark 1, B-3590 Diepenbeek, Belgium
[i] *Prof. Dr. W. Maes*
Department of Chemistry, Molecular Design and Synthesis
KU Leuven
Celestijnenlaan 200F, B-3001 Leuven, Belgium

Supporting information for this article (cyclic voltammograms, TGA and DSC thermal analysis data, XRD pattern of the sublimed Th-DTTzTz material, more details on the computational procedures, and 1H and 13C NMR spectra for all novel thiazolo[5,4-d]thiazole derivatives) is available on the WWW under http://dx.doi.org/10.1002/cplu.200xxxxxx.

Results and Discussion

Synthesis and (electro-optical) characterization

The novel thiazolo[5,4-*d*]thiazole derivatives have been prepared through a convenient three-step synthetic protocol (Scheme 1). The backbone unit, 2,5-bis(3'-hexylthiophene-2'-yl)thiazolo[5,4-*d*]thiazole, was synthesized *via* the classical condensation approach, reacting 3-hexylthiophene-2-carbaldehyde and dithiooxamide.[8,9] After that, a bromination reaction with *N*-bromosuccinimide (NBS) was carried out (in DMF), affording 2,5-bis(5'-bromo-3'-hexylthiophene-2'-yl)thiazolo[5,4-*d*]thiazole (**Br-DTTzTz**). 2,5-Bis(4-hexyl-2,2'-bithiophene-5-yl)thiazolo[5,4-*d*]thiazole (**Th-DTTzTz**) was then obtained through a Stille cross-coupling reaction with tributyl(thiophen-2-yl)stannane ($Pd(PPh_3)_4$, THF).[12] On the other hand, 4-(trifluoromethyl)phenyl-, 4-fluorophenyl- and 4-cyanophenyl-substituted DTTzTz derivatives (**4-CF_3-Ph-DTTzTz**, **4-F-Ph-DTTzTz** and **4-CN-Ph-DTTzTz**) were synthesized through Suzuki cross-coupling reactions with the respective boronic esters ($Pd(PPh_3)_4$, DME, $NaHCO_3$ or K_3PO_4 base). The use of the K_3PO_4 base provided higher yields for the **4-CN-Ph-DTTzTz** compound. All DTTzTz compounds were efficiently purified by column chromatography (on silica) and consecutive recrystallizations, and were isolated as red crystals. The materials were found to be stable under ambient atmosphere at room temperature over a period of several months. Due to the substitution with hexyl side chains, all compounds were nicely soluble in common organic solvents, in particular in chlorinated solvents and ethers.

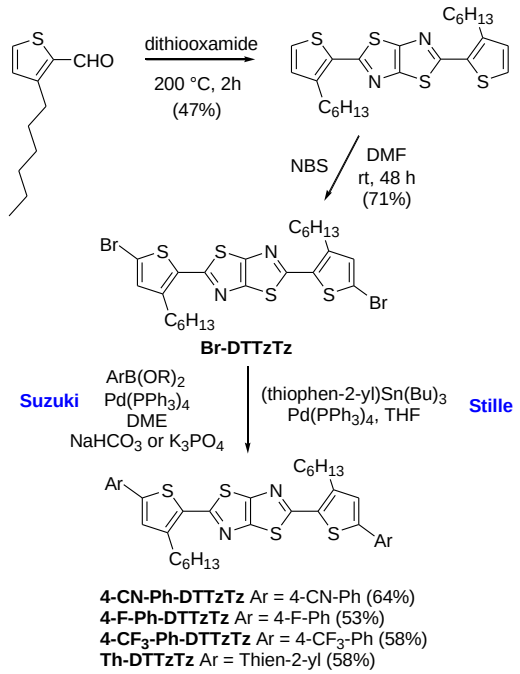

Scheme 1. Synthetic pathway toward soluble 2,5-dithienylthiazolo[5,4-*d*]thiazole derivatives.

Experimental UV-vis absorption maxima (in $CHCl_3$ solution) and cyclic voltammetry (CV) data of the DTTzTz derivatives are summarized in Table 1. For the phenyl-substituted compounds **4-F-Ph-DTTzTz**, **4-CN-Ph-DTTzTz** and **4-CF_3-Ph-DTTzTz**, the absorption maxima were observed at 433, 445 and 434 nm, respectively, somewhat blue-shifted relative to **Th-DTTzTz** (λ_{max}= 449 nm). On the other hand, CV measurements (Figure S1 in the Supporting Info) of **4-F-Ph-DTTzTz**, **4-CN-Ph-DTTzTz** and **4-CF_3-Ph-DTTzTz** revealed oxidation peaks at 0.73, 0.83 and 0.90 V, respectively, notably higher than for **Th-DTTzTz** (0.58 V). These results point to somewhat deeper HOMO levels for the phenyl-substituted materials, suggesting that these compounds might have a higher stability toward oxygen. On the other hand, reduction peaks were found at -1.88, -1.69, -1.89 and -2.01 V for **4-F-Ph-DTTzTz**, **4-CN-Ph-DTTzTz**, **4-CF_3-Ph-DTTzTz** and **Th-DTTzTz**, respectively. Similar CV results concerning the

incorporation of phenyl substituents have been reported before for TzTz-based semiconductors.[13]

Table 1. Optical and electrochemical data for the dithienylthiazolo[5,4-*d*]thiazole derivatives.

DTTzTz	λ_{max} (nm) (log ε)[b]	HOMO[c] (eV)	LUMO[c] (eV)	E_g^{EC} (eV)	E_g^{OP}[d] (eV)
Th[a]	449 (4.768)	-5.51	-2.92	2.59	2.46
4-F-Ph	433 (4.714)	-5.66	-3.05	2.61	2.52
4-CN-Ph	445 (4.777)	-5.76	-3.25	2.51	2.47
4-CF_3-Ph	434 (4.713)	-5.83	-3.04	2.79	2.54

[a] Data taken from previous work.[12] [b] In $CHCl_3$. [c] Evaluated from a CV study in MeCN: 0.1 M Bu_4NPF_6, Pt electrode, scan rate 50 mV s^{-1}. [d] Evaluated from the low energy onset of the absorption spectra in $CHCl_3$.

Table 2. Calculated optical and electrochemical data for the dithienylthiazolo[5,4-*d*]thiazoles as obtained from (TD)DFT calculations.

DTTzTz	λ_{ge} (nm) (f_{ge})[b]	E_g^{OP} (eV)	HOMO (eV)	LUMO (eV)	E_g^{calc} (eV)
Ph[a]	484 (1.91)	2.56	-5.20	-2.28	2.92
Th	516 (1.96)	2.40	-5.10	-2.36	2.74
4-F-Ph	484 (1.91)	2.56	-5.21	-2.30	2.91
4-CN-Ph	508 (2.17)	2.44	-5.45	-2.65	2.80
4-CF_3-Ph	492 (2.00)	2.52	-5.36	-2.48	2.88

[a] The Ph-substituted analogue[11] was merely used as a reference compound for the theoretical calculations and was not included in the OFET study. [b] Oscillator strength.

Density functional theory (DFT) and time-dependent DFT (TDDFT) calculations, summarized in Table 2, supported the experimentally observed changes in optical and electrochemical properties upon replacing the thiophene ring of **Th-DTTzTz** by substituted phenyl groups. In general, the calculated data reflect the experimentally observed trends rather well. The impact of the nature of the terminal aryl moiety on the frontier orbitals and optical band gaps was further exemplified by the topology of the HOMO and LUMO, which are delocalized over the whole backbone (Figure 1 and Figures S2–S5 in the Supporting Info). These differences in optical and electrochemical properties have then been correlated to the Mulliken charge distribution and therefore to the relative electronegativity of the different substituents (Figure 2). So, the smaller/larger optical and electrochemical gaps are associated with more/less positive thiophene donor rings (directly linked to the TzTz core) and less/more positive substituted terminal arenes, in other words, with a better/smaller distribution of the excess positive charge on the 2+2 external ring units, whereas the central TzTz acceptor moiety bears a negative charge.

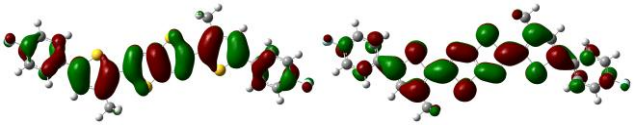

Figure 1. Sketch of the HOMO (left) and LUMO (right) of the most stable conformer of **4-F-Ph-DTTzTz** (hexyl side chains were truncated to methyl groups).

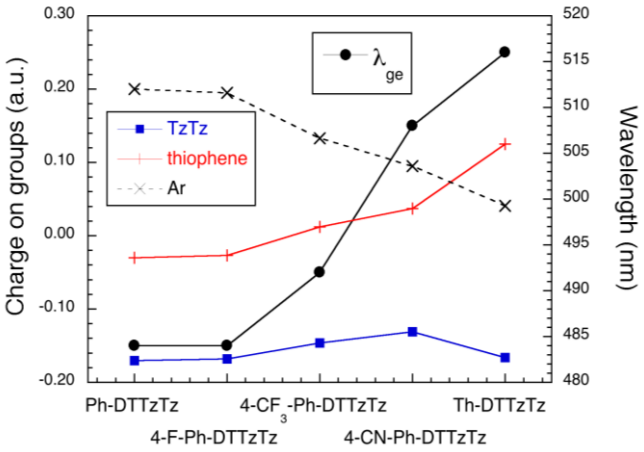

Figure 2. Relationship between the wavelength of absorption of the lowest energy optical transition (λ_{ge}) and the charge distribution on the ring moieties.

Thermal analysis

The DTTzTz moieties were found to be quite thermally stable, as determined by thermogravimetric analysis (TGA), losing less than 1% of their weight on heating up to 400 °C (Figure S6 in the Supporting Info). The thermal properties of the synthesized compounds were further investigated by differential scanning calorimetry (DSC). The DSC results are depicted in Figure 3 (**Th-DTTzTz**) and Figure S7 in the Supporting Info. All derivatives displayed pronounced endothermic and exothermic peaks in heating and cooling, ascribed to melting and crystallization, respectively. **Th-DTTzTz** showed indications of thermally induced side reactions in the DSC experiments. During cooling, crystallization was seen at about 145 °C in the first cycle. These crystals melted at about 177 °C in the subsequent heating. When this cool-heat process was repeated, the crystallization peak shifted to lower temperatures, while the melting peak remained mostly unchanged, except for a shoulder appearing at lower temperatures. The results after five cycles can be seen in Figure 3 (dashed line). This observation can most likely be explained by a limited amount of undesirable side reactions at more elevated temperatures, as virtually no mass loss is observed below 400 °C. For comparison, the non-alkylated analogue showed a single high temperature melting endotherm at 280 °C.[5a] Introduction of a solubilizing alkyl side chain is indeed expected to lower T_m.

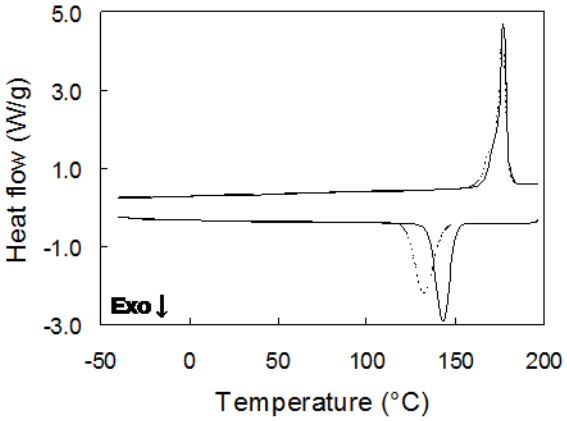

Figure 3. DSC thermogram of **Th-DTTzTz** showing heating and cooling cycles at 20 K min^{-1}. The dashed line shows the result after 5 cycles.

The **4-CF_3-Ph-DTTzTz** material displayed a melting endotherm at 173 °C, whereas the insoluble non-alkylated analogue showed a sharp melting endotherm at 298 °C (Figure S7 in the Supporting Info).[5c] For **4-F-Ph-DTTzTz**, in addition to a melting peak at 188 °C and a crystallization peak at 165 °C, a broad endotherm and exotherm were noted between -10 °C and 60 °C, in both heating and cooling (Figure S7 in the Supporting Info). This might be ascribed to a transition between a liquid crystalline and crystalline form. Finally, the **4-CN-Ph-DTTzTz** compound exhibited a sharp exotherm at 161 °C during cooling, in addition to crystallization at 193 °C, adding up to about 54 J g^{-1}. Upon heating, two very small endothermic peaks were followed by a large melting peak, adding up to 58 J g^{-1}. At a slower cooling rate of 5 K min^{-1}, the exotherm at 161 °C disappeared, but the exothermal enthalpy remained 54 J g^{-1}. The sharp exotherm at 161 °C probably corresponds to the formation of a less stable polymorph that reorganizes to a more stable form upon heating (Figure S7 in the Supporting Info). In summary, although the four synthesized DTTzTz compounds have the same core structure, their crystallization and melting behavior showed significant differences and is complicated by polymorphism and/or liquid crystalline transitions. The considerably higher transition enthalpy in heating for **Th-DTTzTz** (50 kJ mol^{-1}) as compared to the other DTTzTz compounds (22 kJ mol^{-1} for **4-CF_3-Ph-DTTzTz**, 29 kJ mol^{-1} for **4-F-Ph-DTTzTz**, and 39 kJ mol^{-1} for **4-CN-Ph-DTTzTz**) points to a higher crystallinity for **Th-DTTzTz** (Table S1 in the Supporting Info).

Solution-processed OFET characteristics

Subsequently, the electronic and morphological properties of solution-casted thin films of the functionalized TzTz semiconducting materials were investigated, with the goal to obtain good OFET characteristics. Transistor performance was mainly evaluated by the thin film hole mobility (μ) extracted in the saturation regime and by the threshold voltage (V_T), which are listed in Table 3. For the **4-CN-Ph-DTTzTz** derivative, several spin-coating conditions were tested (with optimization of concentration, solvent, spin-coating speed and acceleration), but unfortunately no suitable layers for OFET measurements could be obtained. Although optimized spin-coating conditions were found for **4-CF_3-Ph-DTTzTz** (5 mg mL^{-1} in 1,2-dichlorobenzene, 3000 rpm, 5000 acc, 60 s), hole mobilities of the films calculated in the saturation regime were found to be only around 2×10^{-6} cm^2 V^{-1} s^{-1}. The **4-F-Ph-DTTzTz** material showed a slightly better performance for the same optimized spin-coating conditions, with a calculated hole mobility of 1×10^{-5} cm^2 V^{-1} s^{-1}. On the other hand, the **Th-DTTzTz** semiconductor afforded a noticeably better FET performance with a hole mobility of 1.58×10^{-3} cm^2 V^{-1} s^{-1} (spin-coating conditions: 5 mg mL^{-1} in 1,2-dichlorobenzene, 3000 rpm, 3000 acc, 60 s).

Table 3. Organic field-effect transistor characteristics of bottom contact devices made from the DTTzTz derivatives.

DTTzTz	Hole mobility (μ) (cm^2 V^{-1} s^{-1})	I_{on}/I_{off} Ratio	Threshold Voltage (V_T)
Th	1.58×10^{-3}	10^5	1.4
4-F-Ph	1×10^{-5}	10^4	-3.4
4-CF_3-Ph	2×10^{-6}	10^3	-2.2

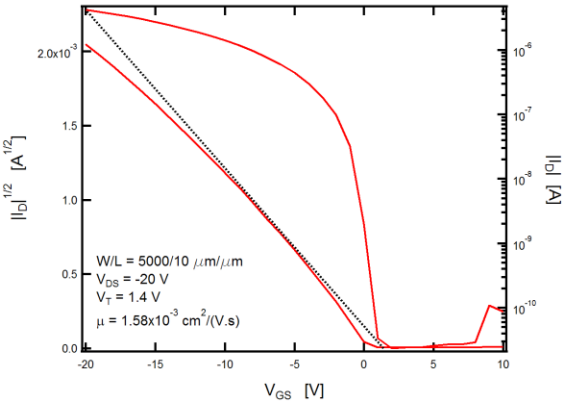

Figure 4. FET characteristics for a bottom contact device made from **Th-DTTzTz**: I_d and $I_d^{1/2}$ versus V_{GS} plots at V_{DS} = –20 V.

Figure 4 shows the obtained transfer characteristics for the **Th-DTTzTz** device, with I_d, V_{DS} and V_{GS} representing the source-drain current, source-drain voltage and gate voltage, respectively. It must be emphasized that, despite the rather poor film-forming characteristics inherent to small molecules, the **Th-DTTzTz** films showed reasonably high hole mobilities. For the analogous non-alkylated Th-DTTzTz material, processed by vacuum deposition, a mobility of 0.02 cm^2 V^{-1} s^{-1} was reported, i.e. one order of magnitude higher.[5e] From a structural point of view, the best result for the **Th-DTTzTz** derivative does not come as a real surprise, as the additional thiophene unit is expected to increase the hole affinity. On the other hand, film morphology and crystallinity also have a major impact on device performance, and the noticeable differences in thermal properties within the DTTzTz series already hinted to large differences in crystallization tendencies.

Morphology studies

To investigate the molecular organization of the DTTzTz molecules on the transistor surface and evaluate a possible correlation with the observed hole mobilities, X-ray diffraction (XRD), atomic force microscopy (AFM) and scanning electron microscopy (SEM) studies were carried out. The observed XRD diffraction patterns are shown in Figure 5. The results were quite similar to earlier reported data for the unsubstituted analogues.[5a,c] The thin films of **Th-DTTzTz** displayed high crystallinity, with a strong primary diffraction peak, pointing to an ordered crystalline structure. This high crystallinity is likely to be the reason for the high hole mobility observed. On the other hand, the crystallinity of the **4-CF$_3$-Ph-DTTzTz** and **4-F-Ph-DTTzTz** derivatives was rather poor, whereas the **4-CN-Ph-DTTzTz** film showed even less evidence of a crystalline phase.

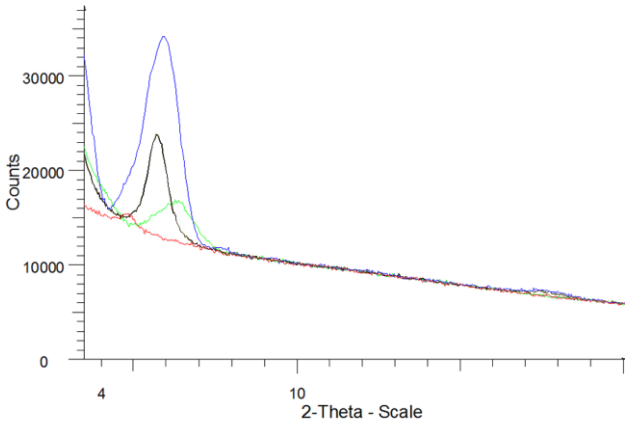

Figure 5. XRD patterns of thin films of **4-CN-Ph-DTTzTz** (15.23 nm, red), 4-**CF$_3$-Ph-DTTzTz** (14.25 nm, green), **4-F-Ph-DTTzTz** (25.75 nm, black) and **Th-DTTzTz** (23.60 nm, blue).

Figures 6 and 7 show optical microscope and SEM images obtained for the different spin-coated films, revealing large differences in morphology. The **Th-DTTzTz** films showed an anisotropic fibrillar morphology (Figure 6). On the other hand, SEM images of solution-processed thin films of **4-CF$_3$-Ph-DTTzTz**, **4-F-Ph-DTTzTz** and **4-CN-Ph-DTTzTz** indicated a very different topography, characterized by the presence of partially connected domains, creating a large number of grain boundaries (Figure 7). These morphologies are in sharp contrast to the one observed for **Th-DTTzTz**, and this profound difference was further confirmed by AFM measurements (Figure 8). The trend in morphology could clearly be correlated to the electrical characteristics: the **4-CF$_3$-Ph-DTTzTz**, **4-F-Ph-DTTzTz** and **4-CN-Ph-DTTzTz** films were characterized by the absence of crystals on the micrometer scale and exhibited quite poor hole mobilities, whereas the high mobility **Th-DTTzTz** film showed a fibrillar microcrystalline texture. The significantly higher hole mobility in this case might be related to the presence of intergranular charge transport paths, as boundaries along the fibrils could provide a smaller barrier to charge transport.[14] The thin films were proven to be (oxidatively) stable, as essentially identical SEM images were obtained after storage for two months.

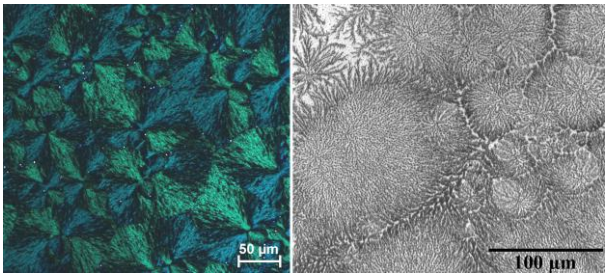

Figure 6. Optical microscope (left) and SEM (right) images of spin-coated thin films of **Th-DTTzTz**.

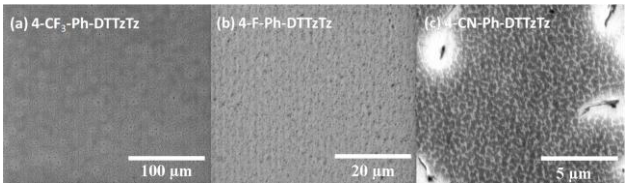

Figure 7. SEM images of thin films of **4-CF$_3$-Ph-DTTzTz**, **4-F-Ph-DTTzTz** and **4-CN-Ph-DTTzTz**.

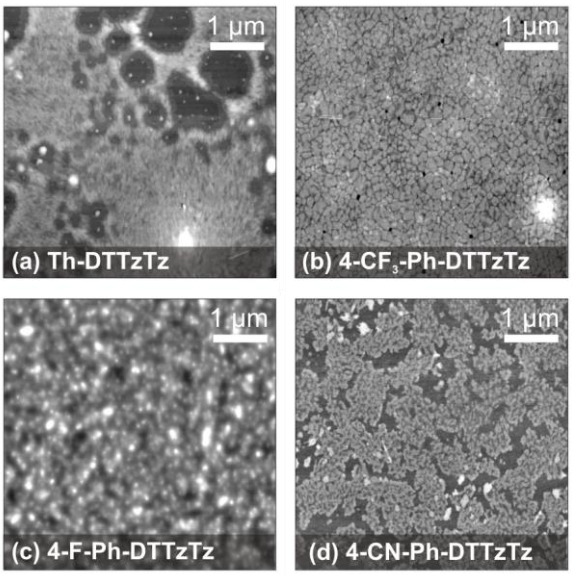

Figure 8. AFM images (5 x 5 µm^2) of spin-coated thin films of the DTTzTz derivatives on SiO_2 with a rms roughness of a) 1.9 nm, b) 0.8 nm, c) 3 nm and d) 1.2 nm.

Vacuum sublimed OFET

For comparison, the most promising molecule from the series, **Th-DTTzTz**, was also deposited by thermal evaporation in an ultra high vacuum chamber at a base pressure below 5×10^{-8} Torr. The temperature of the evaporation cell varied between 200 and 220 °C. Transistors were fabricated and were

subjected to a surface treatment with pentafluorobenzenethiol and deposition of a self-assembling monolayer of phenylethyltrichlorosilane (PETS). The hole mobilities calculated in the saturation regime were found to be 2×10^{-4} cm^2 V^{-1} s^{-1}. Without applying a surface treatment, hole mobilities of only 6×10^{-6} cm^2 V^{-1} s^{-1} were achieved. The hole mobility of 1.58×10^{-3} cm^2 V^{-1} s^{-1} generated in the solution-processed OFET's could hence not be reached by vacuum deposition of the same material. Although XRD studies showed a high degree of crystallinity in the vacuum deposited films (Figure S8 in the Supporting Info), the SEM images revealed a high number of grain boundaries due to the presence of a large amount of nanosized domains (Figure 9). These nanocrystals probably result in a reduced mobility as compared to the fibrillar microcrystals obtained after spin-coating. Furthermore, it cannot be excluded that side reactions occurring during vacuum deposition of the **Th-DTTzTz** material between 200 and 220 °C (compared to the much "softer" conditions for solution processing), as observed in the DSC experiment (Figure 3), might also be (partly) responsible for this reduced mobility.

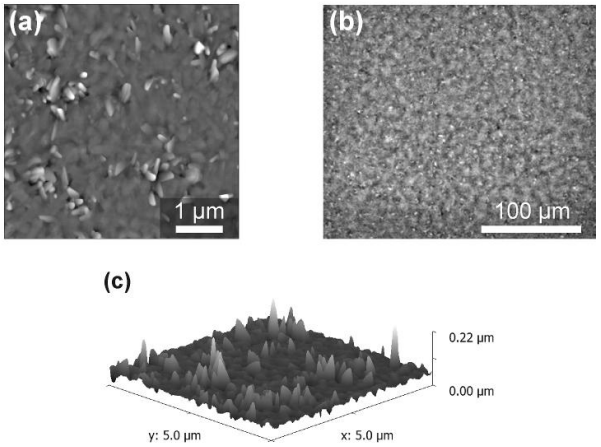

Figure 9. Vacuum sublimed **Th-DTTzTz** film imaged by a) AFM (5 x 5 μm^2), displaying a rms roughness of 14 nm, b) SEM, c) 3D AFM.

Conclusion

Aiming for small organic compounds suitable for printable electronics, we have synthesized a family of highly soluble 2,5-dithienylthiazolo[5,4-*d*]thiazole semiconducting materials by a convenient three-step protocol, and studied their thermal, optical and electrochemical properties. FET devices were fabricated from these materials by spin-coating active layers from solutions in dichlorobenzene. Despite some difficulties in film formation, the bithiophene-substituted TzTz material (**Th-DTTzTz**) exhibited a fairly high hole mobility of $1.58\text{x}10^{-3}$ cm^2 V^{-1} s^{-1}, making it a suitable candidate for solution-processable organic field-effect transistors. The alkyl-substituted **Th-DTTzTz** showed better self-organization when deposited from solution compared to vacuum deposited layers, resulting in higher hole mobilities. This higher mobility might be linked to the microcrystalline fibrillar structure observed for the solution-casted film, whereas vacuum deposition of the same material afforded a film with multiple nanocrystalline domains. These results clearly show the major effects of both (subtle) structural modifications in organic semiconducting materials and the applied processing conditions on final device performances.

Experimental Section

Materials and Methods

Unless stated otherwise, all reagents and chemicals were obtained from commercial sources and used without further purification. NMR chemical shifts (δ, in ppm) were determined relative to the residual $CHCl_3$ absorption (7.24 ppm) or the ^{13}C resonance shift of $CDCl_3$ (77.7 ppm). Mass spectra were run using a Thermo Finnigan LCQ Advantage apparatus (electrospray ionization, ESI). Solution UV/Vis absorption measurements were performed at a scan rate of 600 nm min^{-1} in a continuous run from 200 to 800 nm. Infrared spectra were collected with a resolution of 4 cm^{-1} (16 scans) using films drop-casted on a NaCl disk from a $CHCl_3$ solution. The XRD measurements were performed with a Bruker D8 discover diffractometer under *θ-2θ* conditions. The system works in parafocusing geometry using a Göbel mirror (line focus, mostly $CuK\alpha_1$ and $CuK\alpha_2$ rays). The X-rays are detected by a 1D detector. Electrochemical measurements were performed with an Eco Chemie Autolab PGSTAT 30 potentiostat/galvanostat using 0.1 M Bu_4NPF_6 in anhydrous MeCN as the electrolyte under N_2 atmosphere. A three-electrode microcell was utilized containing an $Ag/AgNO_3$ reference electrode (0.1 M $AgNO_3$ and 0.1 M Bu_4NPF_6 in MeCN), a platinum counter electrode and an indium tin oxide (ITO) coated glass substrate as the working electrode. The respective monomers were dissolved to their maximum solubility in the electrolyte solution. Cyclic voltammograms were recorded at a scan rate of 50 mV s^{-1}. For the conversion to eV, all electrochemical potentials were referenced to a known standard (ferrocene/ferrocenium in MeCN, 0.05 V *vs.* $Ag/AgNO_3$), which in MeCN solution is estimated to have an oxidation potential of -4.98 V *vs.* vacuum. DSC measurements were performed at 20 K min^{-1} in aluminum crucibles on a TA Instruments Q2000 Tzero DSC equipped with a refrigerated cooling system (RCS), using nitrogen (50 mL min^{-1}) as a purge gas. TGA experiments were performed at 50 K min^{-1} in platinum crucibles on a TA Instruments Q5000 TGA using nitrogen (50 mL min^{-1}) as a purge gas. FET transistors were made on a highly doped Si n^{++} common gate substrate on which 120 nm SiO_2 was thermally grown. Afterwards, Au source/drain bottom contacts were defined by a lift-off process. The measured transistors had a channel width (W) of 5000 µm and a channel length (L) of 10 µm. Substrate cleaning consisted of subsequent rinsing with detergent, deionized water and acetone, followed by submersion in isopropanol. Finally, a 15 min UV-O_3 treatment was applied prior to depositing the nicely soluble compounds at room temperature by spin-coating. The FET characteristics were then determined inside a glove box under N_2 atmosphere with a Hewlett Packard Agilent 4156. SEM images were recorded with a FEI Quanta 200 FEG scanning electron microscope. The topography of the spin-coated and sublimed films was

studied by AFM, using a Picoscan PicoSPM LE scanning probe microscope in tapping mode.

Synthesis

2,5-Bis(5'-bromo-3'-hexylthiophene-2'-yl)thiazolo[5,4-d]thiazole (**Br-DTTzTz**) was synthesized according to a previously reported procedure.[12] Material identity and purity were confirmed by mp, MS, ^{1}H and ^{13}C NMR.

2,5-Bis(4-hexyl-2,2'-bithiophene-5-yl)thiazolo[5,4-d]thiazole (**Th-DTTzTz**) was synthesized according to a previously reported procedure.[12] Material identity and purity were confirmed by mp, MS, ^{1}H and ^{13}C NMR.

4,4,5,5-Tetramethyl-2-[4-(trifluoromethyl)phenyl]-1,3,2-dioxaborolane was synthesized according to a literature procedure.[15] Material identity and purity were confirmed by MS and ^{1}H NMR.

2-(4-Fluorophenyl)-4,4,5,5-tetramethyl-1,3,2-dioxa-borolane was synthesized according to a literature procedure.[16] Material identity and purity were confirmed by MS and ^{1}H NMR.

4-(4,4,5,5-Tetramethyl-1,3,2-dioxaborolan-2-yl)benzonitrile was synthesized according to a literature procedure.[16] Material identity and purity were confirmed by MS and ^{1}H NMR.

2,5-Bis[5'-(4-fluorophenyl)-3'-hexylthiophen-2'-yl]-thiazolo[5,4-d]thiazole (**4-F-Ph-DTTzTz**). **General procedure**. A solution of 2-(4-fluorophenyl)-4,4,5,5-tetramethyl-1,3,2-dioxaborolane (0.480 g, 1.76 mmol) in DME (15 mL) was added dropwise to a stirring mixture of 2,5-bis(5'-bromo-3'-hexylthiophene-2'-yl)thiazolo[5,4-*d*]thiazole (0.450 g, 0.706 mmol) and $Pd(PPh_3)_4$ (0.033 g, 28 µmol) in DME (20 mL) at ambient temperature. Subsequently, a $NaHCO_3$ solution (1 M, 25 mL) was added. After stirring for 24 h at 60 °C under N_2 atmosphere and protected from light, the reaction mixture was diluted with water (50 mL). The organic layer was separated and the aqueous layer was extracted with $CHCl_3$ (3 x 50 mL). The combined organic layers were washed with a saturated $NaHCO_3$ solution and brine, dried over $MgSO_4$ and concentrated by evaporation *in vacuo*. The reaction product was purified by column chromatography (silica, eluent hexane/ethyl acetate 95:5) and recrystallized from ethanol, resulting in red crystals of pure **4-F-Ph-DTTzTz** (0.250 g, 53%). ^{1}H NMR (300 MHz, $CDCl_3$, 25°C): δ = 7.60 (dd, *J*(H,H) = 9/6 Hz, 4H), 7.08 (t, *J*(H,H) = 9 Hz, 4H), 7.12 (s, 2H), 2.94 (t, *J*(H,H) = 8 Hz, 4H), 1.79–1.69 (m, 4H), 1.49–1.43 (m, 4H), 1.37–1.32 (m, 8H), 0.90 ppm (t, *J*(H,H) = 7 Hz, 6H); ^{13}C NMR (75 MHz, $CDCl_3$, 25°C): δ = 163.6, 161.9, 150.9, 145.2, 144.9, 131.9, 130.7, 128.3 (CH), 127.4 (CH), 116.8 (CH), 32.4 (CH_2), 31.1 (CH_2), 30.7 (CH_2), 30.1 (CH_2), 23.3 (CH_2), 14.8 ppm (CH_3); UV/Vis ($CHCl_3$): λ_{max} (log ε) = 433 nm (4.714); MS (ESI): *m/z* = 663 [*M*H$^+$].

2,5-Bis(3'-hexyl-5'-[4-(trifluoromethyl)phenyl]thio-phen-2'-yl)thiazolo[5,4-d]thiazole (**4-CF$_3$-Ph-DTTzTz**). Synthesis according to the general procedure: 4,4,5,5-tetramethyl-2-[4-(trifluoromethyl)phenyl]-1,3,2-dioxaborolane (1.076 g, 3.96 mmol), 2,5-bis(5'-bromo-3'-hexylthiophene-2'-yl)thiazolo[5,4-*d*]thiazole (1.00 g, 1.58 mmol), $Pd(PPh_3)_4$ (0.073 g, 63 µmol), DME (20 + 80 mL), $NaHCO_3$ (1 M, 65 mL); 0.698 g of red crystals (58% yield). ^{1}H NMR (300 MHz, $CDCl_3$, 25°C): δ = 7.73 (d, *J*(H,H) = 9 Hz, 4H), 7.64 (d, *J*(H,H) = 9 Hz, 4H), 7.27 (s, 2H), 2.97 (t, *J*(H,H) = 8 Hz, 4H), 1.81–1.71 (m, 4H), 1.49–1.45 (m, 4H), 1.38–1.33 (m, 8H), 0.90 ppm (t, *J*(H,H) = 6.9 Hz, 6H); ^{13}C NMR (75 MHz, $CDCl_3$, 25°C): δ = 161.5, 150.9, 144.7, 143.9, 137.3, 133.0, 130.4, 128.3 (CH), 126.6 (CH), 126.2 (CH), 124.7, 32.3 (CH_2), 31.2 (CH_2), 30.4 (CH_2), 30.1 (CH_2), 23.3 (CH_2), 14.8 ppm (CH_3); UV/Vis ($CHCl_3$): λ_{max} (log ε) = 434 nm (4.713); MS (ESI): *m/z* = 763 [*M*H$^+$].

4,4'-[5,5'-(Thiazolo[5,4-d]thiazole-2,5-diyl)-bis(4-hexylthiophene-5,2-diyl)]dibenzonitrile (**4-CN-Ph-DTTzTz**). Synthesis according to the general procedure: 4-(4,4,5,5-tetramethyl-1,3,2-dioxaborolan-2-yl)benzonitrile (0.420 g, 1.83 mmol), 2,5-bis(5'-bromo-3'-hexylthiophene-2'-yl)thiazolo[5,4-*d*]thiazole (0.230 g, 0.367 mmol), $Pd(PPh_3)_4$ (0.017 g, 15 µmol), DME (20 + 50 mL), K_3PO_4 (0.260 g, 1.25 mmol), eluent hexane/$CHCl_3$ 20:80; 0.159 g of red crystals (64% yield). ^{1}H NMR (300 MHz, $CDCl_3$, 25°C): δ = 7.72 (d, *J*(H,H) = 9 Hz, 4H), 7.67 (d, *J*(H,H) = 9 Hz, 4H), 7.30 (s, 2H), 2.96 (t, *J*(H,H) = 7.8 Hz, 4H), 1.80–1.70 (m, 4H), 1.50–1.45 (m, 4H), 1.37–1.32 (m, 8H), 0.90 ppm (t, *J*(H,H) = 6.9 Hz, 6H); ^{13}C NMR (75 MHz, $CDCl_3$, 25°C): δ = 161.6, 151.3, 145.0, 143.5, 138.3, 133.8, 133.5 (CH), 129.2 (CH), 126.6 (CH), 119.3, 112.0, 32.3 (CH_2), 31.1 (CH_2), 30.5 (CH_2), 30.1 (CH_2), 23.3 (CH_2), 14.8 ppm (CH_3); IR (NaCl): ν_{max} = 2956/2925/2855 (s, saturated C-H), 2220 cm^{-1} (m, CN); UV/Vis ($CHCl_3$) λ_{max} (log ε) = 445 nm (4.777); MS (ESI): *m/z* = 677 [*M*H$^+$].

Acknowledgements

The authors gratefully acknowledge the IWT (Institute for the Promotion of Innovation by Science and Technology in Flanders) for financial support via the SBO-project 060843 "PolySpec". We also acknowledge the European ONE-P project for grant agreement n° 212311 which facilitates the IMEC-IMOMEC collaboration. Furthermore, we gratefully thank BELSPO in the frame of the IAP-VII FS2 network as well as MINCyT and FRS-FNRS for supporting the Buenos Aires-Namur scientific cooperation. The computational calculations were performed on the Interuniversity Scientific Computing Facility (ISCF) installed at the Facultés Universitaires Notre-Dame de la Paix (FUNDP, Namur, Belgium), for which we acknowledge financial support from the FRS-FRFC (Convention No. 2.4.617.07.F) and from the FUNDP. V. L. thanks the FRS-FNRS for his postdoctoral research position. N. VdB. and W. M. thank the FWO (Fund for Scientific Research – Flanders) for a doctoral and postdoctoral research mandate, respectively.

Keywords: organic field-effect transistors • conducting materials • thiazolo[5,4-*d*]thiazoles • substituent effects • thin film morphology • printable electronics

[1] a) M. Muccini, *Nat. Mater.* **2006**, *5*, 605; b) L. Locklin, M. E. Roberts, S. C. B. Mannsfeld, Z. Bao, *J. Macromol. Sci., Part C: Polym. Rev.* **2006**, *46*, 79; c) C.-a. Di, G. Yu, Y. Liu, D. Zhu, *J. Phys. Chem. B* **2007**, *111*, 14083; d) D. Braga, G. Horowitz, *Adv. Mater.* **2009**, *21*, 1473; e) Y. Yamashita, *Sci. Technol. Adv. Mater.* **2009**, *10*, 024313; f) H. Seirringhaus, M. Bird, T. Richards, N. Zhao, *Adv. Mater.* **2010**, *22*, 3893; g) W. Wu, Y. Liu, D. Zhu, *Chem. Soc. Rev.* **2010**, *39*, 1489; h) M. J. Malachowski, J. Zmija, *Opto-Electron. Rev.* **2010**, *18*, 121; i) A. Operamolla, G. M. Farinola, *Eur. J. Org. Chem.* **2011**, 423.

[2] a) L. Duan, L. Hou, T.-W. Lee, J. Qiao, D. Zhang, G. Dong, L. Wang, Y. Qiu, *J. Mater. Chem.* **2010**, *20*, 6392; b) C. Zhong, C. Duan, F. Huang, H. Wu, Y. Cao, *Chem. Mater.* **2011**, *23*, 326.

[3] a) H. M. Ko, H. Choi, S. Paek, K. Kim, K. Song, J. K. Lee, J. Ko, *J. Mater. Chem.* **2011**, *21*, 7248; b) H. Shang, H. Fan, Y. Liu, W. Hu, Y. Li, X. Zhan, *Adv. Mater.* **2011**, *23*, 1554; c) Y. Sun, G. C. Welch, W. L. Leong, C. J. Takacs, G. C. Bazan, A. J. Heeger, *Nat. Mater.* **2012**, *11*, 44.

[4] a) M. Ashizawa, R. Kato, Y. Takanishi, H. Takezoe, *Chem. Lett.* **2007**, *36*, 708; b) K. Haubner, E. Jaehne, H.-J. P. Adler, D. Koehler, C. Loppacher, L. M. Eng, J. Grenzer, A. Herasimovich, S. Scheinert, *Phys. Stat. Sol.* **2008**, *205*, 431; c) M. Mass-Torrent, C. Rovira, *Chem. Soc. Rev.* **2008**, *37*, 827; d) Y. Liu, G. Yu, Y. Liu, *Sci. China Chem.* **2010**, *53*, 779; e) L. Zhang, C.-a. Di, G. Yu, Y. Liu, *J. Mater. Chem.* **2010**, *20*, 7059.

[5] a) S. Ando, J.-i. Nishida, Y. Inoue, S. Tokito, Y. Yamashita, *J. Mater. Chem.* **2004**, *14*, 1787; b) S. Ando, J.-i. Nishida, E. Fujiwara, H. Tada, Y. Inoue, S. Tokito, Y. Yamashita, *Chem. Lett.* **2004**, *33*, 1170; c) S. Ando, J.-i. Nishida, H. Tada, Y. Inoue, S. Tokito, Y. Yamashita, *J. Am. Chem. Soc.* **2005**, *127*, 5336; d) S. Ando, J.-i. Nishida, E. Fujiwara, H. Tada, Y. Inoue, S. Tokito, Y. Yamashita, *Synth. Met.* **2006**, *156*, 327; e) S. Ando, D. Kumaki, J.-i. Nishida, H. Tada, Y. Inoue, S. Tokito, Y. Yamashita, *J. Mater. Chem.* **2007**, *17*, 553; f) D. Kumaki, S. Ando, S. Shimono, Y. Yamashita, *Appl. Phys. Lett.* **2007**, *90*, 53506; g) M. Mamada, J.-i. Nishida, D. Kumaki, S. Tokito, Y. Yamashita, *Chem. Mater.* **2007**, *19*, 5404. h) Y. Fujisaki, M. Mamada, D. Kumaki, S. Tokito, Y. Yamashita, *Jpn. J. Appl. Phys.* **2009**, *48*, 111504.

[6] Naraso, F. Wudl, *Macromolecules* **2008**, *41*, 3169.

[7] a) I. Osaka, G. Sauvé, R. Zhang, T. Kowalewski, R. D. McCullough, *Adv. Mater.* **2007**, *19*, 4160; b) I. Osaka, R. Zhang, G. Sauvé, D.-M. Smilgies, T. Kowalewski, R. D. McCullough, *J. Am. Chem. Soc.* **2009**, *131*, 2521; c) I. Osaka, R. Zhang, J. Liu, D.-M. Smilgies, T. Kowalewski, R. D. McCullough, *Chem. Mater.* **2010**, *22*, 4191.

[8] J. R. Johnson, R. Ketcham *J. Am. Chem. Soc.* **1960**, *82*, 2719.

[9] J. R. Johnson, D. H. Rotenberg, R. Ketcham, *J. Am. Chem. Soc.* **1970**, *92*, 4046.

[10] a) T. W. Lee, N. S. Kang, J. W. Yu, M. H. Hoang, K. H. Kim, J.-L. Jin, D. H. Choi, *J. Polym. Sci., Part A: Polym. Chem.* **2010**, *48*, 5921; b) I. H. Jung, J. Yu, E. Jeong, J. Kim, S. Kwon, H. Kong, K. Lee, H. Y. Woo, H.-K. Shim, *Chem. Eur. J.* **2010**, *16*, 3743; c) L. Huo, X. Guo, S. Zhang, Y. Li, J. Hou, *Macromolecules* **2011**, *44*, 4035; d) S. K. Lee, J. M. Cho, Y. Goo, W. S. Shin, J.-C. Lee, W.-H. Lee, I.-N. Kang, H.-K. Shim, S.-J. Moon, *Chem. Commun.* **2011**, 1791; e) S. K. Lee, I.-N. Kang, J.-C. Lee, W. S. Shin, W.-W. So, S.-J. Moon, *J. Polym. Sci., Part A: Polym. Chem.* **2011**, *49*, 3129; f) T. W. Lee, N. S. Kang, J. W. Yu, M. H. Hoang, K. H. Kim, J.-I. Jin, D. H. Choi, *J. Polym. Sci., Part A: Polym. Chem.* **2011**, *49*, 5921; g) J. Peet, L. Wen, P. Byrne, S. Rodman, K. Forberich, Y. Shao, N. Drolet, R. Gaudiana, G. Dennler, D. Waller, *Appl. Phys. Lett.* **2011**, *98*, 043301; h) S. Subramaniyan, H. Xin, F. S. Kim, S. Shoaee, J. R. Durrant, S. A. Jenekhe, *Adv. Energy Mater.* **2011**, *1*, 854; i) S. Subramaniyan, H. Xin, F. S. Kim, S. A. Jenekhe, *Macromolecules* **2011**, *44*, 6245; j) M. Zhang, X. Guo, X. Wang, H. Wang, Y. Li, *Chem. Mater.* **2011**, *23*, 4264; k) M. Helgesen, M. V. Madsen, B. Andreasen, T. Tromholt, J. W. Andreasen, F. C. Krebs, *Polym. Chem.* **2011**, *2*, 2536; l) E. Jeong, G.-h. Kim, I. H. Jung, P. Jeong, J. Y. Kim, H. Y. Woo, *Curr. Appl. Phys.* **2012**, *12*, 11; m) I. Osaka, M. Saito, H. Mori, T. Koganezawa, K. Takimiya, *Adv. Mater.* **2012**, *24*, 425; n) S. Van Mierloo, A. Hadipour, M.-J. Spijkman, N. Van den Brande, B. Ruttens, J. Kesters, J. D'Haen, G. Van Assche, D. M. de Leeuw, T. Aernouts, J. Manca, L. Lutsen, D. J. Vanderzande, W. Maes, *Chem. Mater.* **2012**, *24*, 587.

[11] We have recently reported a combined experimental-theoretical NMR study on a number of 2,5-bis(5'-aryl-3'-hexylthiophen-2'-yl)thiazolo[5,4-*d*]thiazole derivatives: S. Van Mierloo, V. Liégeois, J. Kudrjasova, E. Botek, L. Lutsen, B. Champagne, D. Vanderzande, P. Adriaensens, W. Maes, *Magn. Reson. Chem.* **2012**, *50*, 379.

[12] S. Van Mierloo, S. Chambon, A. E. Boyukbayram, P. Adriaensens, L. Lutsen, T. J. Cleij, D. Vanderzande, *Magn. Reson. Chem.* **2010**, *48*, 362.

[13] X. M. Hong, H. E. Katz, A. J. Lovinger, B.-C. Wang, K. Raghavachari, *Chem. Mater.* **2001**, *13*, 4686.

[14] L. H. Jimison, M. F. Toney, I. McCulloch, M. Heeney, A. Salleo, *Adv. Mater.* **2009**, *21*, 1568.

[15] J. Cremer, E. Mena-Osteritz, N. G. Pschierer, K. Müllen, P. Bäuerle, *Org. Biomol. Chem.* **2005**, *3*, 985.

[16] T. Ishiyama, M. Murata, N. Miyaura, *J. Org. Chem.* **1995**, *60*, 7508.

Received:
Published online:

Entry for the Table of Contents

FULL PAPER

A series of dithienylthiazolo[5,4-*d*]thiazole (DTTzTz) semiconductors was synthesized and investigated as active materials in solution-processed OFET's. Spin-coated films of one of the derivatives showed a micrometer scale fibrillar texture and high field-effect mobilities (10^{-3} cm^2 V^{-1} s^{-1}) were observed. This molecule represents the first example of a highly soluble DTTzTz-based small organic compound for which a reasonable FET behavior was observed.

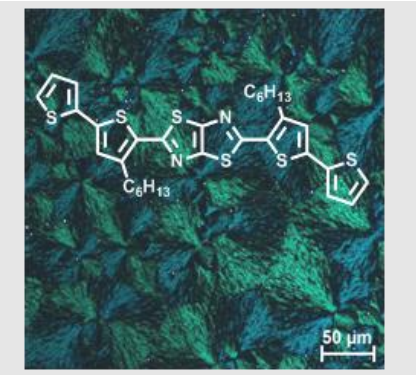

Sarah Van Mierloo, Karolien Vasseur, Niko Van den Brande, Ayse E. Boyukbayram, Bart Ruttens, Silvio D. Rodriguez, Edith Botek, Vincent Liégeois, Jan D'Haen, Peter J. Adriaensens, Paul Heremans, Benoît Champagne, Guy Van Assche, Laurence Lutsen, Dirk J. Vanderzande, and Wouter Maes**

Functionalized Dithienylthiazolo[5,4-d]thiazoles for Solution-Processable Organic Field-Effect Transistors

Supporting Information

Functionalized Dithienylthiazolo[5,4-*d*]thiazoles for Solution-Processable Organic Field-Effect Transistors

Sarah Van Mierloo,[a] Karolien Vasseur,[b] Niko Van den Brande,[c] Ayse E. Boyukbayram,[a],[d] Bart Ruttens,[e] Silvio D. Rodriguez,[f],[g] Edith Botek,[f] Vincent Liégeois,[f] Jan D'Haen,[e] Peter J. Adriaensens,[a] Paul Heremans,[b] Benoît Champagne,[f] Guy Van Assche,[c] Laurence Lutsen,[h] Dirk J. Vanderzande,* [a],[h] and Wouter Maes* [a],[i]

Table of contents

1. Cyclic voltammograms of Th-DTTzTz, 4-F-Ph-DTTzTz, 4-CN-Ph-DTTzTz and 4-CF_3-Ph-DTTzTz

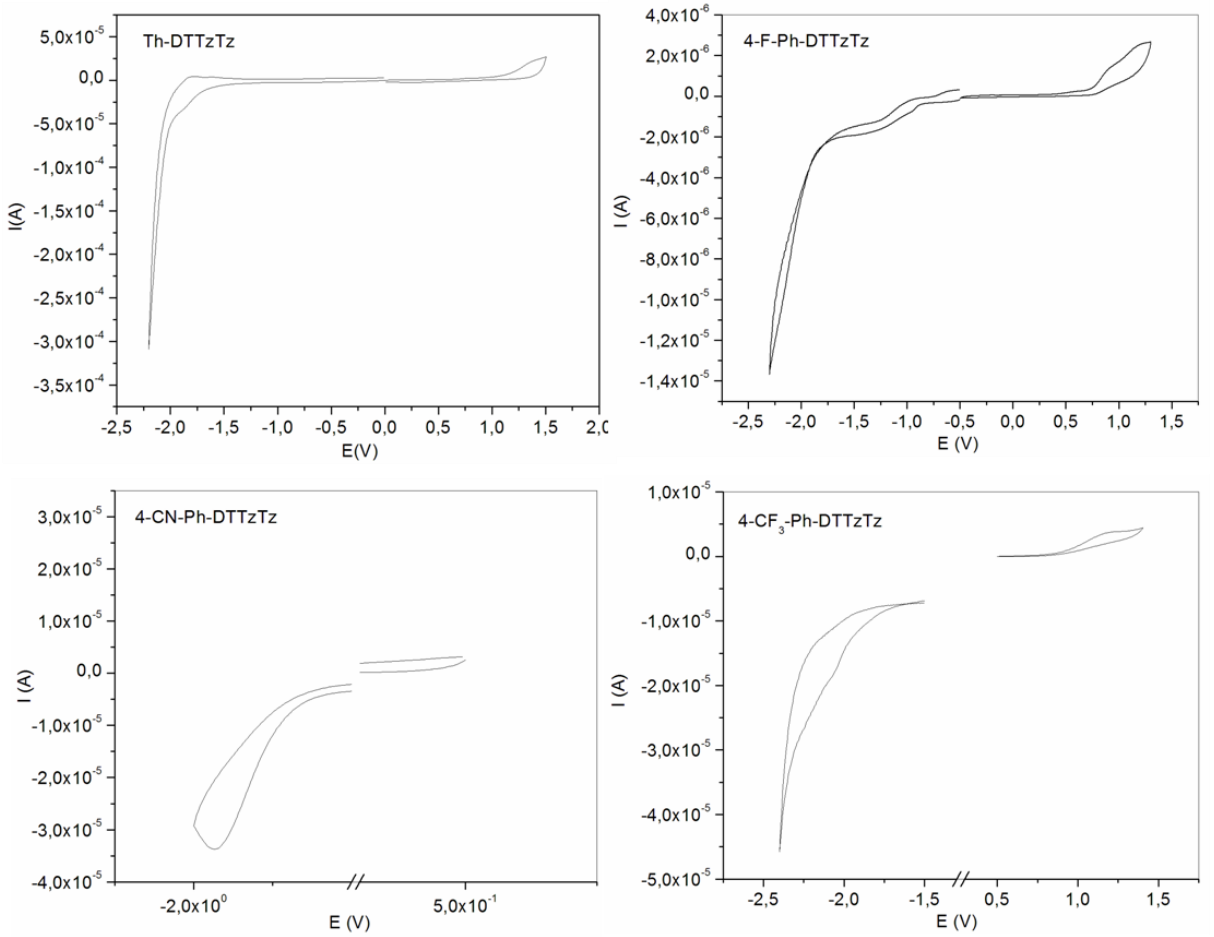

Figure S1. Cyclic voltammograms of **Th-DTTzTz**, **4-F-Ph-DTTzTz**, **4-CN-Ph-DTTzTz** and **4-CF_3-Ph-DTTzTz**.

2. Theoretical and computational data

The ground state geometries were optimized at the density functional theory (DFT) level of approximation by employing the B3LYP exchange-correlation (XC) functional and the 6-31G(d) basis set. These geometries and wave functions were employed to analyze the shape of the Highest Occupied and Lowest Unoccupied Molecular Orbitals (HOMO and LUMO).

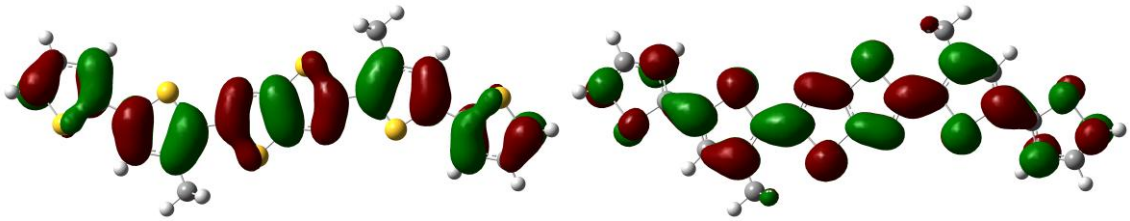

Figure S2. Sketch of the HOMO (left) and LUMO (right) of the most stable conformer of **Th-DTTzTz** (hexyl side chains were truncated to methyl groups).

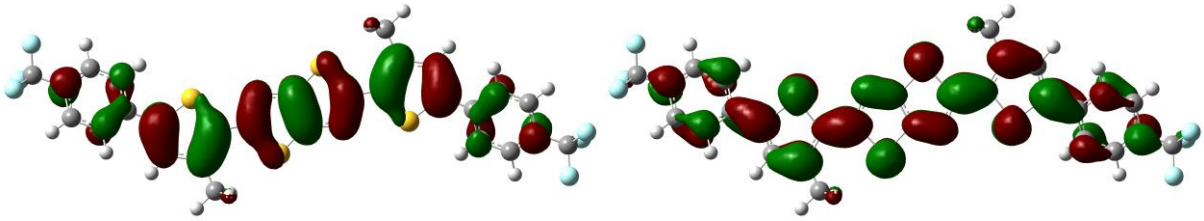

Figure S3. Sketch of the HOMO (left) and LUMO (right) of the most stable conformer of **4-CF_3-Ph-DTTzTz** (hexyl side chains were truncated to methyl groups).

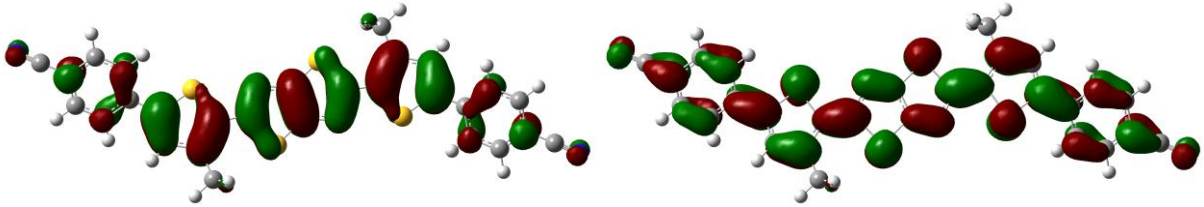

Figure S4. Sketch of the HOMO (left) and LUMO (right) of the most stable conformer of **4-CN-Ph-DTTzTz** (hexyl side chains were truncated to methyl groups).

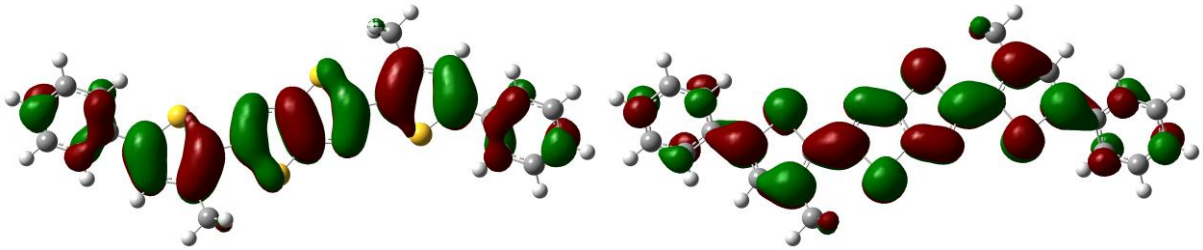

Figure S5. Sketch of the HOMO (left) and LUMO (right) of the most stable conformer of **Ph-DTTzTz** (hexyl side chains were truncated to methyl groups).

The vertical excitation energies ΔE_{ge}, wavelengths λ_{ge}, and associated oscillator strengths f_{ge} were calculated using time-dependent DFT (TDDFT) with the same XC functional containing 20% of HF exchange and the same basis set, which has been shown to be a suitable method for reproducing experimental trends.[1] The effects of the solvent were taken into account within the integral equation formalism of the polarizable continuum model (IEF-PCM)[2] in the geometry optimization as well as to carry out the Mulliken population analysis. All calculations were performed using Gaussian09.[3]

[1] a) V. Cavillot, B. Champagne, *Chem. Phys. Lett.* **2002**, *354*, 449; b) M. Guillaume, B. Champagne, F. Zutterman, *J. Phys. Chem. A* **2006**, *110*, 13007; c) A. Plaquet, M. Guillaume, B. Champagne, L. Rougier, F. Mançois, V. Rodriguez, J. L. Pozzo, L. Ducasse, F. Castet, *J. Phys. Chem. C* **2008**, *112*, 5638.

[2] a) J. Tomasi, M. Persico, *Chem. Rev.* **1994**, *94*, 2027; b) J. Tomasi, B. Mennucci, R. Cammi, *Chem. Rev.* **2005**, *105*, 2999.

[3] Gaussian 09, Revision A.1, M. J. Frisch, G. W. Trucks, H. B. Schlegel, G. E. Scuseria, M. A. Robb, J. R. Cheeseman, G. Scalmani, V. Barone, B. Mennucci, G. A. Petersson, H. Nakatsuji, M. Caricato, X. Li, H. P. Hratchian, A. F. Izmaylov, J. Bloino, G. Zheng, J. L. Sonnenberg, M. Hada, M. Ehara, K. Toyota, R. Fukuda, J. Hasegawa, M. Ishida, T. Nakajima, Y. Honda, O. Kitao, H. Nakai, T. Vreven, Jr. J. A. Montgomery, Jr. J. E. Peralta, F. Ogliaro, M. Bearpark, J. J. Heyd, E. Brothers, K. N. Kudin, V. N. Staroverov, R. Kobayashi, J. Normand, K. Raghavachari, A. Rendell, J. C. Burant, S. S. Iyengar, J. Tomasi, M. Cossi, N. Rega, J. M. Millam, M. Klene, J. E. Knox, J. B. Cross, V. Bakken, C. Adamo, J. Jaramillo, R. Gomperts, R. E. Stratmann, O. Yazyev, A. J. Austin, R. Cammi, C. Pomelli, J. W. Ochterski, R. L. Martin, K. Morokuma, V. G. Zakrzewski, G. A. Voth, P. Salvador, J. J. Dannenberg, S. Dapprich, A. D. Daniels, Ö. Farkas, J. B. Foresman, J. V. Ortiz, J. Cioslowski, D. J. Fox, Gaussian, Inc., Wallingford CT, **2009**.

3. Thermal analysis data

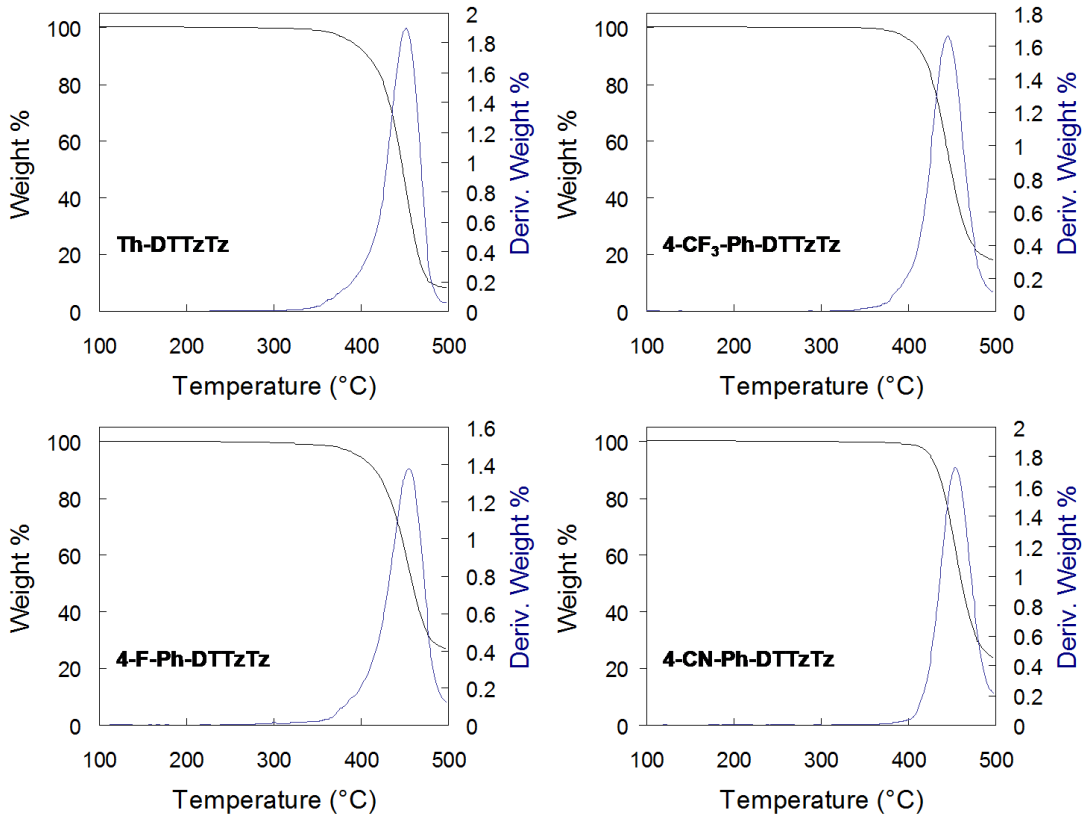

Figure S6. TGA curves of **Th-DTTzTz**, **4-CF_3-Ph-DTTzTz**, **4-F-Ph-DTTzTz** and **4-CN-Ph-DTTzTz** (heating rate 50 K min^{-1}, N_2 atmosphere).

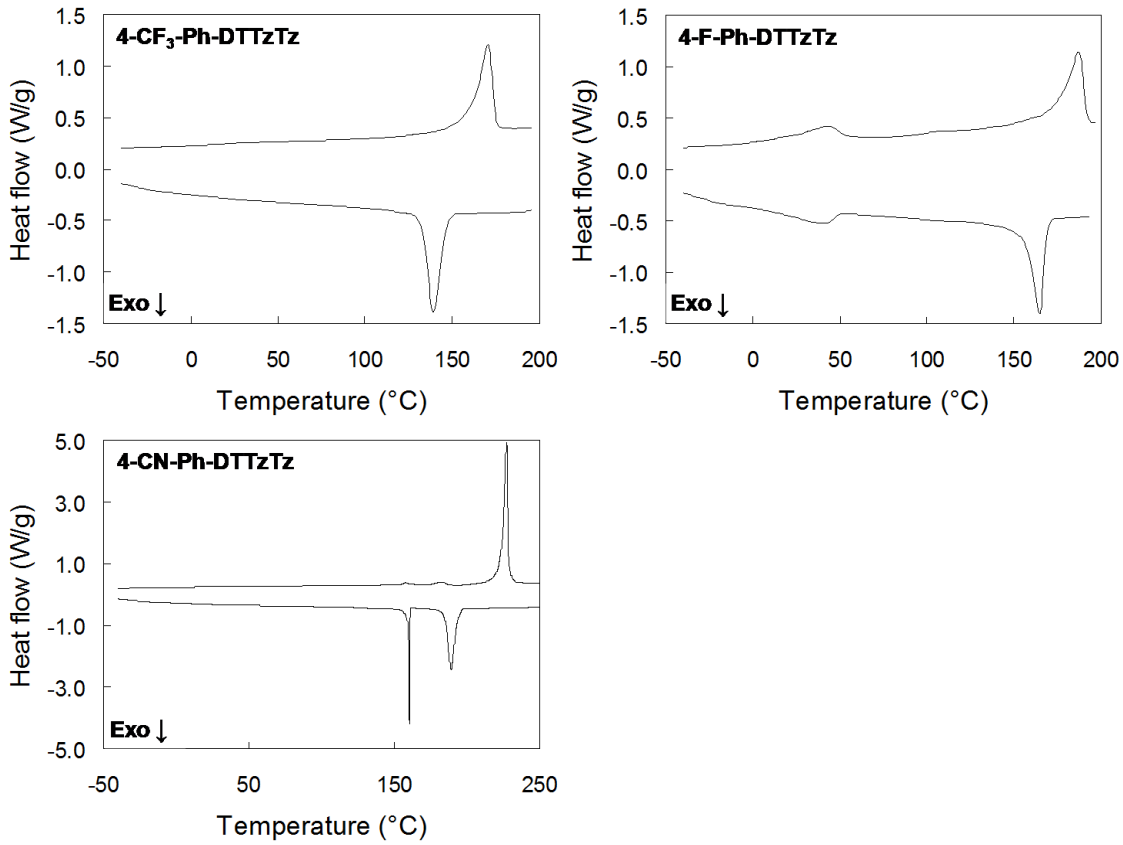

Figure S7. DSC thermograms of **4-CF_3-Ph-DTTzTz**, **4-F-Ph-DTTzTz** and **4-CN-Ph-DTTzTz**, showing heating and cooling cycles at 20 K min^{-1}.

Table S1. Extrapolated onset temperatures and transition enthalpies *ΔH* for the first cool-heat cycles given in Figure 3 and Figure S7.

		T_{onset} (°C)	*ΔH* (J g^{-1})	*ΔH* (kJ mol^{-1})
Th-DTTzTz	cool	149.9	72.6	46.4
	heat	172.9	78.7	50.3
4-CF_3-Ph-DTTzTz	cool	147.7	28.7	21.9
	heat	160.5	29.3	22.4
4-F-Ph-DTTzTz	cool	49.7	11.2	7.4
	cool	169.2	29.6	19.6
	heat	12.2	12.1	8.0
	heat	173.7	31.4	20.8
	cool	161.0	16.7	11.3
4-CN-Ph-DTTzTz	cool	193.0	37.5	25.4
	heat	224.5	58.2	39.4

4. XRD pattern of the sublimed Th-DTTzTz semiconductor

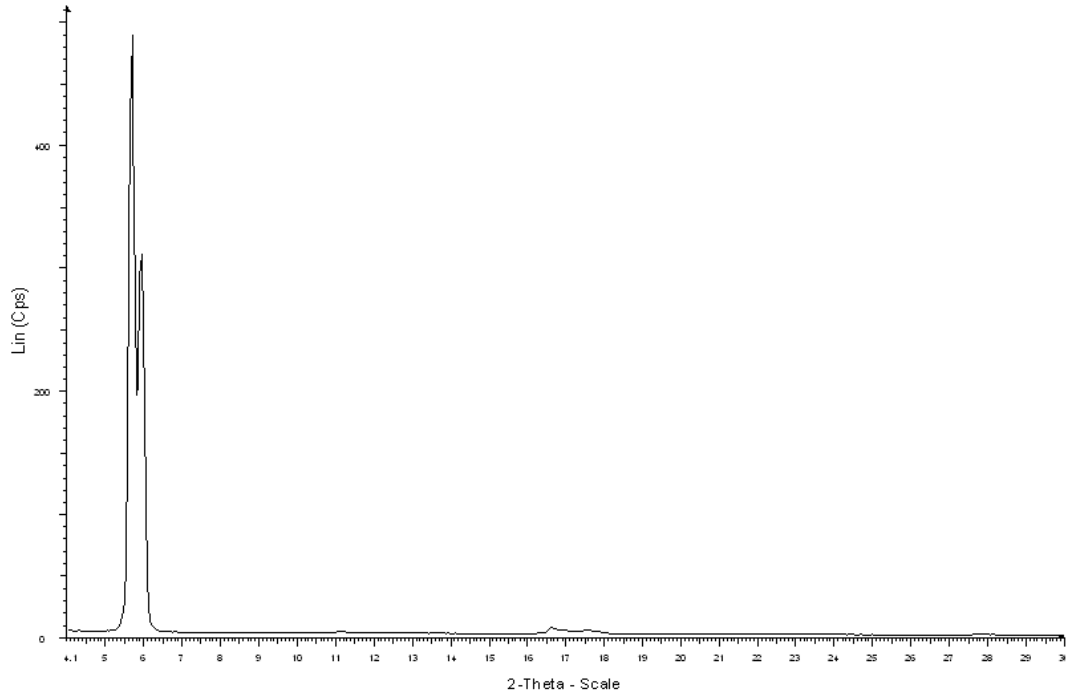

Figure S8. XRD pattern of the sublimed **Th-DTTzTz** material.

5. ^{1}H (300 MHz, $CDCl_3$) and ^{13}C (75 MHz, $CDCl_3$) NMR spectra for the novel DTTzTz's

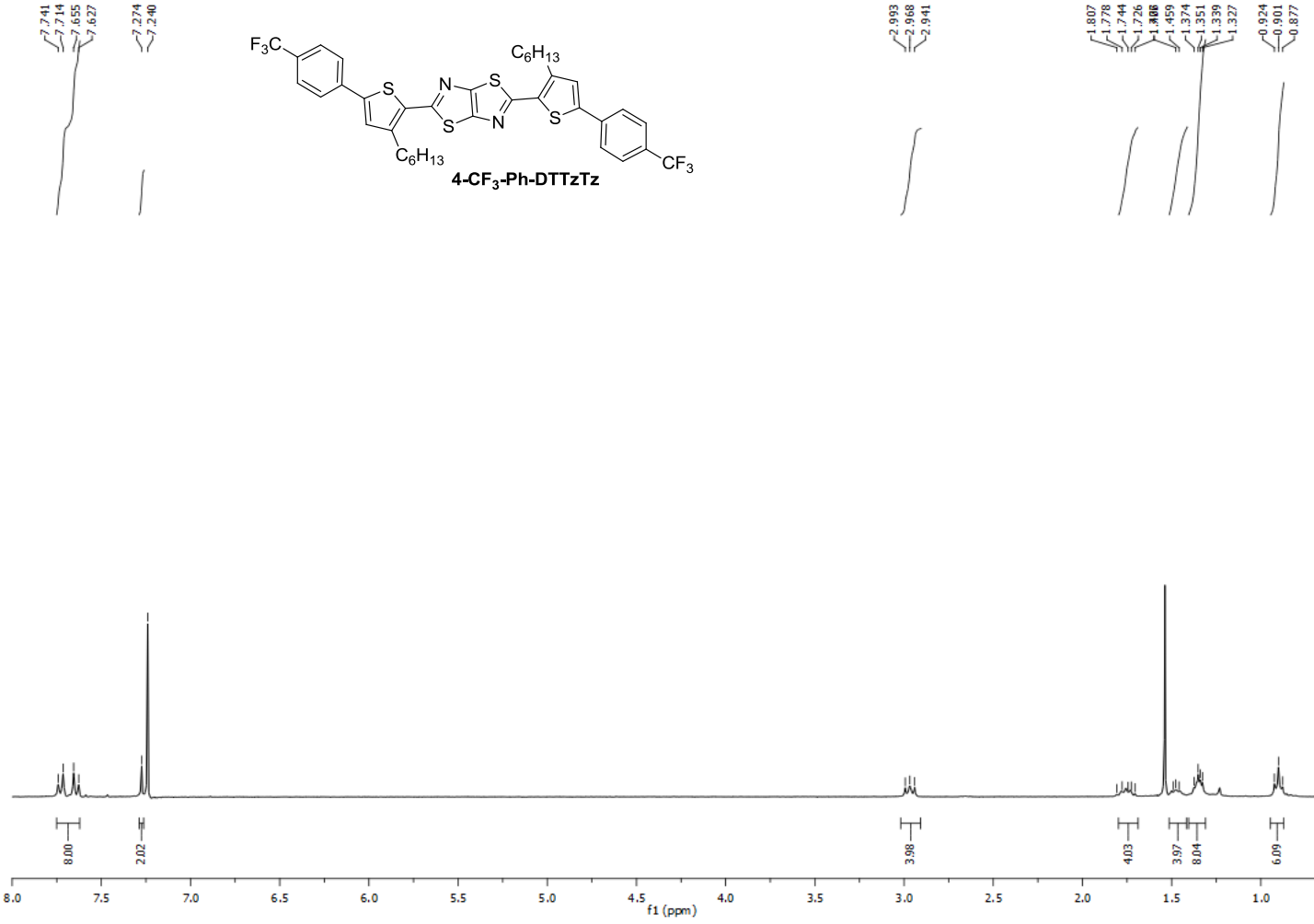

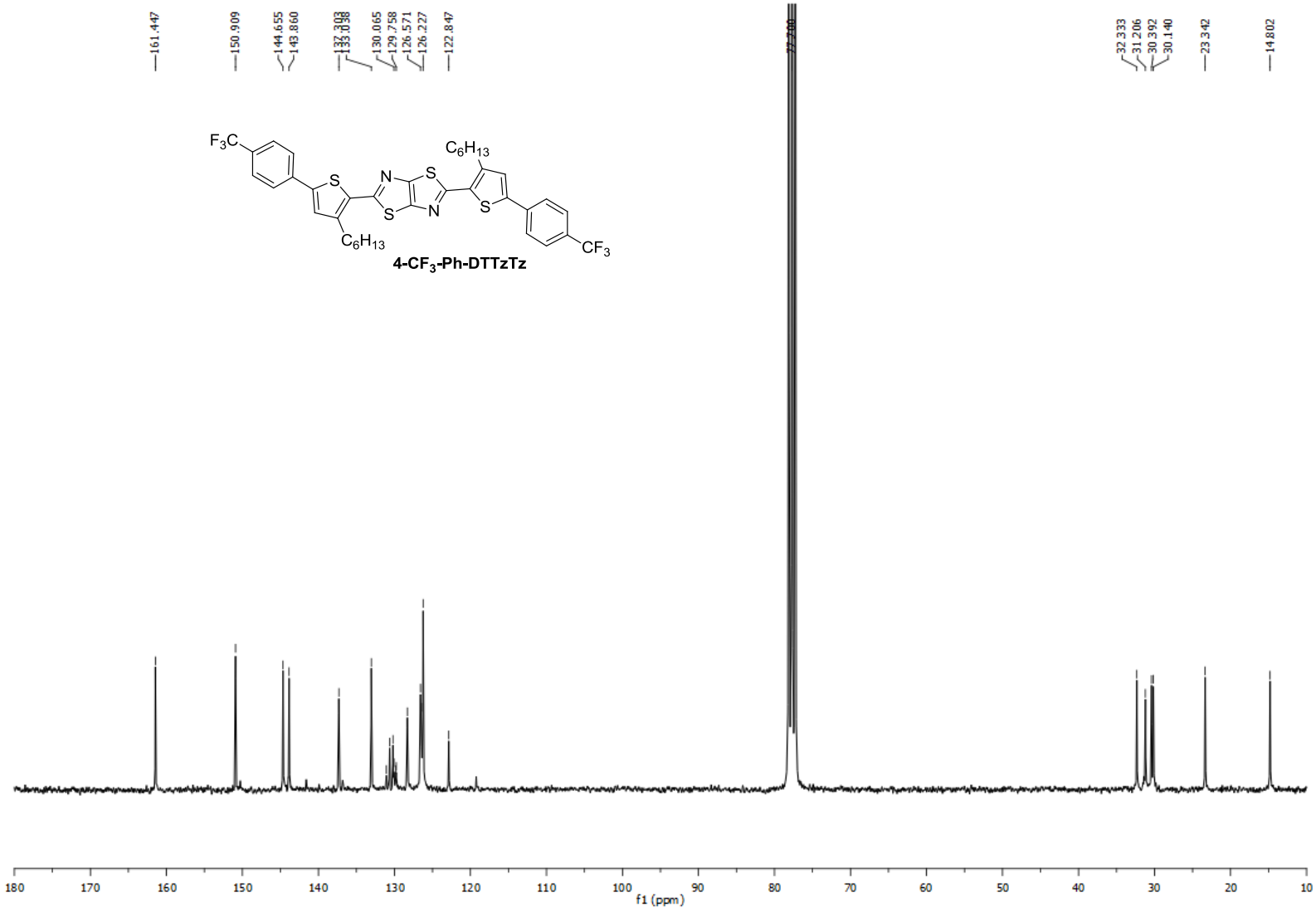
161.447
150.909
144.655
143.860
137.303
133.038
130.065
129.758
126.571
126.227
122.847
77.200
32.333
31.206
30.392
30.140
23.342
14.802
F3C
C6H13
C6H13
CF3
S
N
S
S
N
S
4-CF3-Ph-DTTzTz
180
170
160
150
140
130
120
110
100
90
80
70
60
50
40
30
20
10
f1 (ppm)

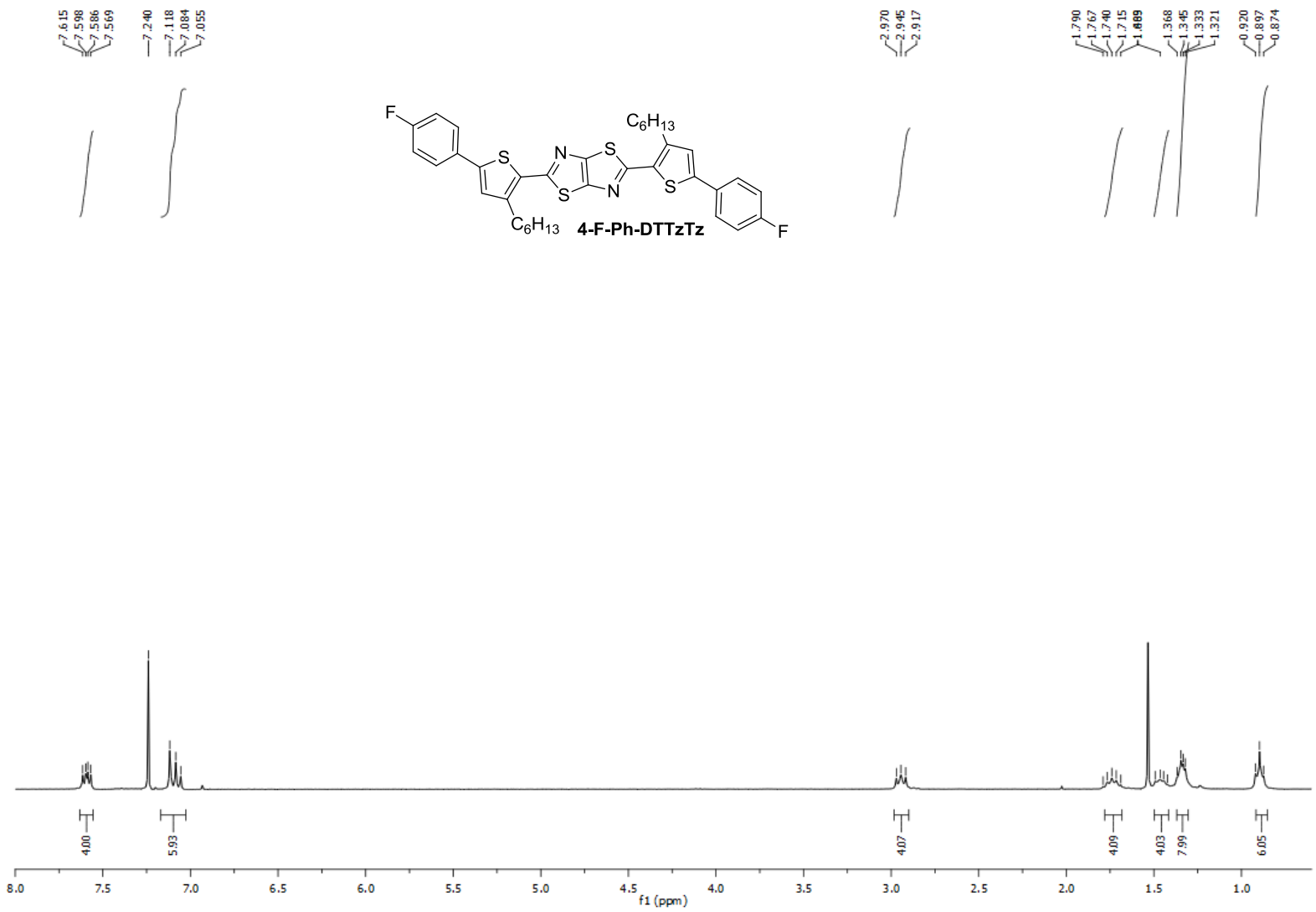
7.615
7.598
7.586
7.569
7.240
7.118
7.084
7.055
2.970
2.945
2.917
1.790
1.767
1.740
1.715
1.368
1.345
1.333
1.321
0.920
0.897
0.874
F
S
N
S
N
S
S
C6H13
C6H13
F
4-F-Ph-DTTzTz
4.00
5.93
4.07
4.09
4.03
7.99
6.05
8.0
7.5
7.0
6.5
6.0
5.5
5.0
4.5
4.0
3.5
3.0
2.5
2.0
1.5
1.0
f1 (ppm)

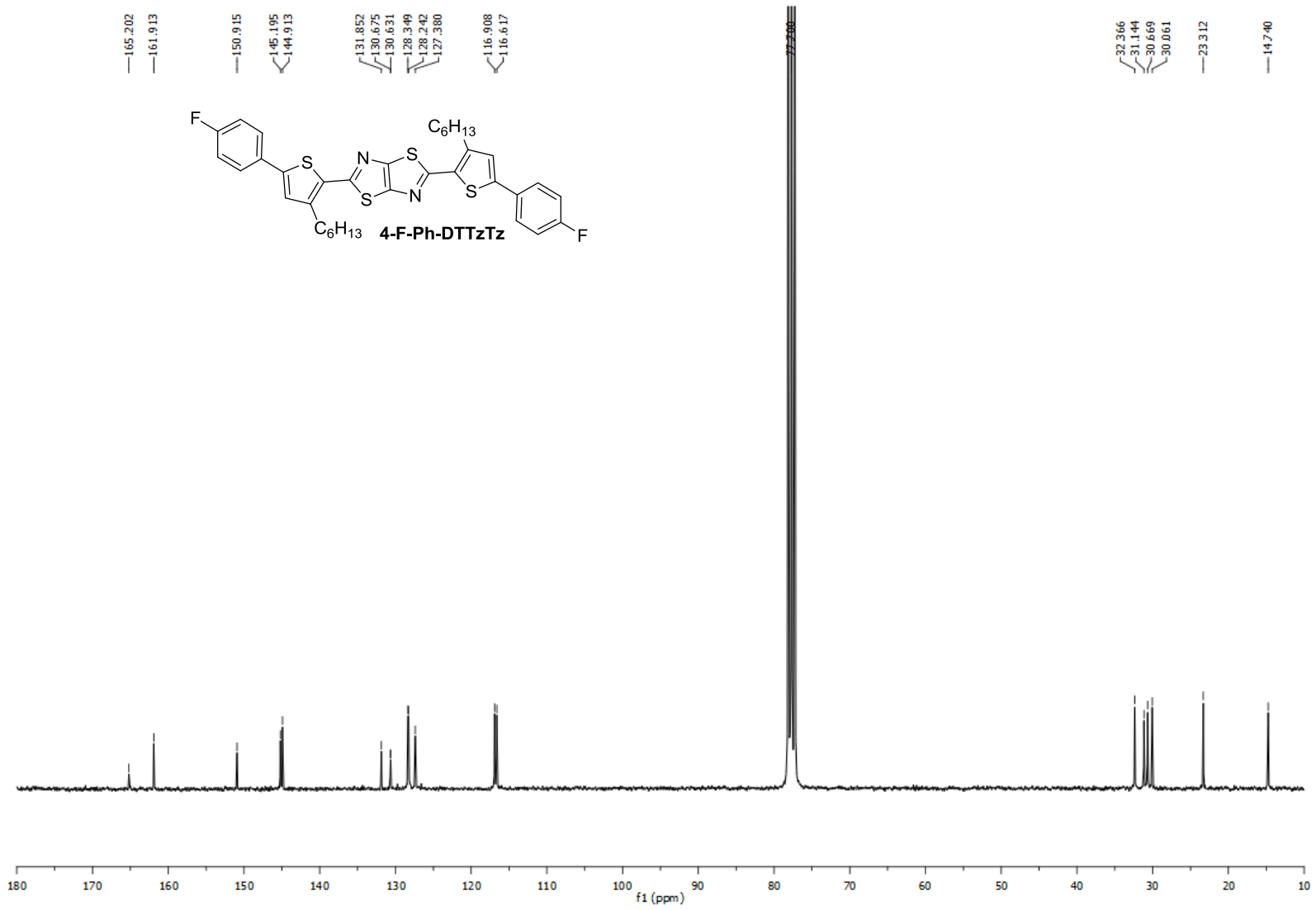
165.202
161.913
150.915
145.195
144.913
131.852
130.675
130.631
128.349
128.242
127.380
116.908
116.617
77.200
32.366
31.144
30.669
30.061
23.312
14.740
F
S
N
S
S
N
S
C6H13
C6H13
F
4-F-Ph-DTTzTz
180
170
160
150
140
130
120
110
100
90
80
70
60
50
40
30
20
10
f1 (ppm)

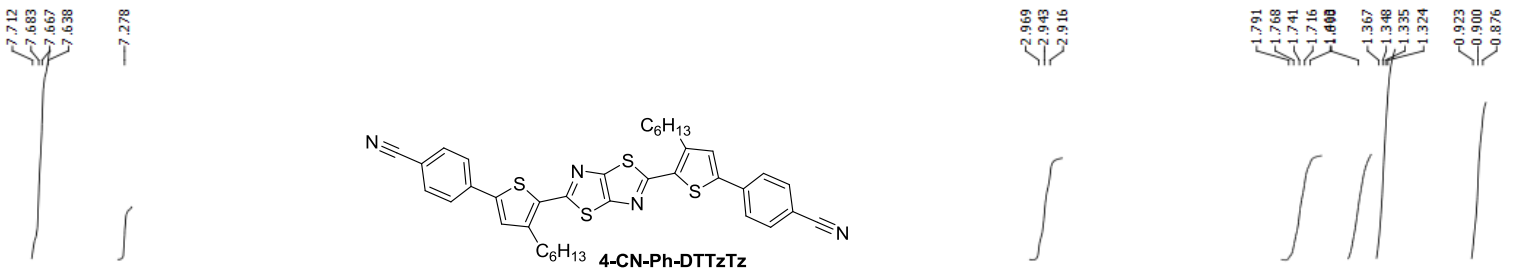

4-CN-Ph-DTTzTz

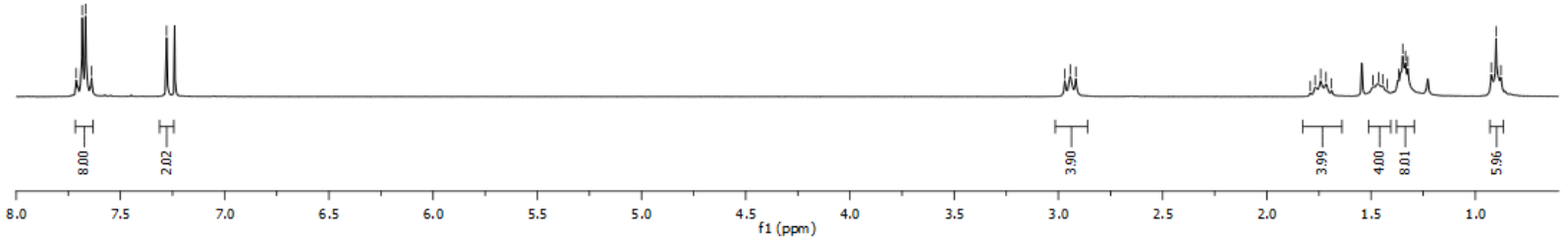

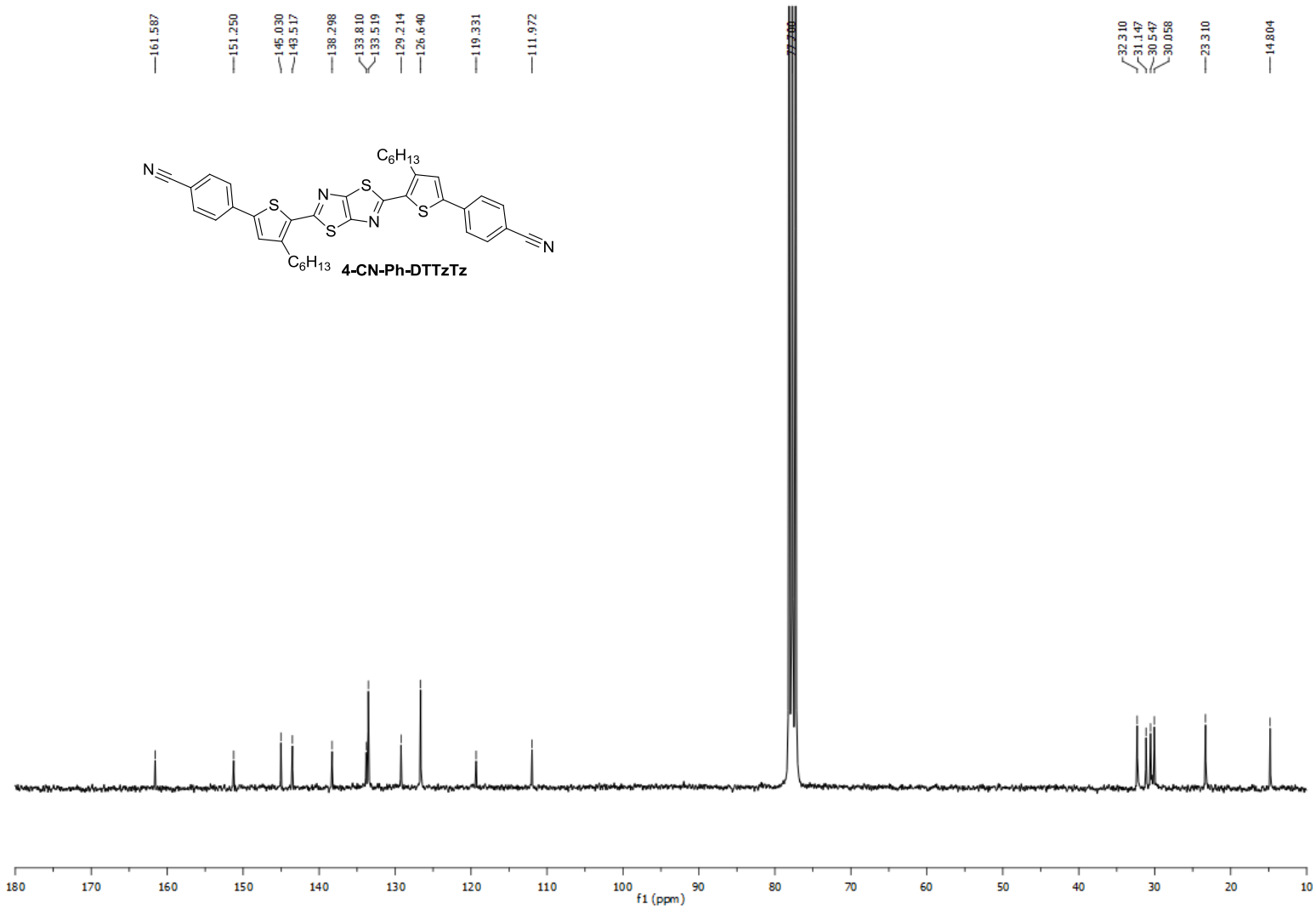
161.587
151.250
145.030
143.517
138.298
133.810
133.519
129.214
126.640
119.331
111.972
77.200
32.310
31.147
30.547
30.058
23.310
14.804
N
S
N
S
N
S
S
C_6H_{13}
C_6H_{13}
N
4-CN-Ph-DTTzTz
180
170
160
150
140
130
120
110
100
90
80
70
60
50
40
30
20
10
f1 (ppm)